Low-temperature synthesis of copper conductivity film from a copper formate amine complex with a low boiling point

Akihiro Yabuki,[1]* Sayuri Kawahara,[1] Soonchul Kang,[1] and Indra Wahyudhin Fathona[2]

[1]Department of Chemical Engineering, Graduate School of Engineering, Hiroshima University, 1-4-1 Kagamiyama, Higashi-hiroshima, 739-8527, Japan

[2]Physics Engineering Department, Electrical Engineering Faculty, Telkom University Terusan Telekomunikasi, Dayeuh Kolot Bandung, 40257, Indonesia

*Corresponding author. Tel/fax: +81 82 424 7852

E-mail address: ayabuki@hiroshima-u.ac.jp (A. Yabuki)

Abstract:

A low-temperature synthesis of copper conductive film was conducted at the near-decomposition-onset temperature of copper formate-amine complex inks. Amines with a low boiling point (butylamine (b.p. 78 ˚C), pentylamine (b.p. 104 ˚C), and hexylamine (b.p. 132 ˚C)) were mixed with copper formate to prepare the complex inks, followed by calcination at various temperatures. The copper film calcined from copper-pentylamine complex ink showed the lowest level of resistivity. The optimal molar ratio for the conversion of pentylamine to copper formate was set at 2.4. That ratio resulted in a volume resistivity of 5.7 μΩ cm following calcination at 110 ˚C. The composition of the copper film was dominated by three sizes of nanoparticles, which were generated via a two-step formation of nanoparticles.

Keywords: onset temperature; amines; complex ink; conductive film; copper

1. Introduction

Electronic devices are trending toward compact, portable, flexible, and wearable. These characteristics have been intensively developed via the development of devices that include flexible electrodes [1–8], fabric-based printed circuits [9–15], and bio-sensors [16–21]. Xu et al. gather the information of metal thin film for flexible electrode which resulted in the thickness varied from 50 μm below [1]. Direct printing using inks has been a key technology for the development of the devices, because it allows conductive, semiconductive, and insulating films or lines to be applied to various substrates. One of the prescribed properties for the inks is low-temperature fabrication, which depends on the thermal stability of flexible polymeric substrates such as polyimide, polyethylene terephthalate (PET), polycarbonate, polypropylene, and polyethylene. Polyimide film is generally used as a flexible substrate because of its high thermal stability. Various polymers with low thermal stability, however, such as polycarbonate (120-130 ºC) and polyethylene (90-110 ºC), would be applicable as flexible substrates due to cost competitiveness.

The fabrication of copper conductive film via printing methods has been reported using nanoparticle and copper complex inks. In research involving copper conductive film using nanoparticles, conductive film from the agglomeration of 5 nm copper nanoparticles sintered at 250 ºC have shown a resistivity of 4.37 x 10^{-6} Ω cm [22]. Copper nanoparticles (20 nm) have been used to prepare electrical conductive films with thickness varied from 0.8 to 1.51 μm, and copper nanoparticle films calcined under air and then hydrogen gas at 200 °C have shown a low resistivity of 2 x 10^{-5} Ω cm [23]. Thus, the calcination temperature is generally high in the fabrication of copper film using nanoparticles, since the sintering between nanoparticles is limited.

There are many reports of conductive films synthesized by thermal decomposition using copper complex ink for low-temperature fabrication. Copper film fabricated from copper

formate ink at 250 ºC shows a volume resistivity of 1.5 x 10^{-5} Ω cm, which has thickness of 0.9 μm [24]. Ink derived from copper and organic sources has been applied to printing using a roll-to-roll process onto a flexible substrate, which results in volume resistivities of 1.0 x 10^{-5} and 4.4 x 10^{-6} Ω cm via calcinations at 250 and 320 °C, respectively [25]. Conductive film fabricated via the spray pyrolysis of a copper-silver amine ink complex has resulted in a volume resistivity of 19 x 10^{-6} Ω cm at 200 °C [26]. Zhang et. al. fabricated Cu film from Cu-Ethyl complex/metal nanowire inks by sintering process at temperature140 ºC, resulted in lowest resistivity of 14.9 x 10^{-6} Ω cm [27]. The thickness varied from 8.7-9.4 mm. Copper film (thickness 5-15 μm) fabricated from complex ink consisting of copper formate and blended amine with different alkyl chain lengths, which resulted in a synergetic effect, and the copper-butyl-octyl amine ink calcined at 200 ºC indicated a resistivity of 4.28 x 10^{-6} Ω cm [28]. Copper film on a polyimide substrate by thermal decomposition of copper complex ink at 180 ºC resulted in thickness of 1.1-1.3 μm and a volume resistivity of 1.8 x 10^{-5} Ω cm [29]. Copper conductive film was synthesized via the thermal decomposition of a copper-octylamine complex, and when calcined above 110 °C, the film indicated electrical conductivities, resulting in the lowest resistivity of 2 x 10^{-5} Ω cm at 140 °C, which has thickness of 200 μm [30]. Copper films fabricated from complexes of copper formate and various amines consisted of copper nanoparticles, the conductivity and nanoparticle size of which depended on the types of amines and their alkyl chain lengths, resulting in blended amines of octylamine and dibutylamine that produced lower levels of resistivity reaching 5.0 x 10^{-6} Ω cm at 140 °C [23,30–33]. Copper film fabricated from copper-pyridine complex ink resulted in a resistivity of 1.4 x10^{-5} Ω cm after sintering at 135 °C [34]. Thus, the use of copper-amine complex inks allows a reduction in temperature during the fabrication of copper films. The lowest temperature reported has been 110 °C, but the conductivity was insufficient [31]. This was caused by problems that included both insufficient decomposition and amine

residue following calcination. Fabricating copper films at lower temperatures requires selecting the correct amine and the correct calcination temperature.

In the present study, copper conductive films were synthesized at lower temperatures from complex inks of copper formate and various amines. In order to fabricate copper conductive films at a lower temperature, we focused on calcination that approached decomposition onset temperature and on the selection of amines with a low boiling point that would avoid residue impurities. The formation process of copper film was elucidated via surface observation by SEM and via analysis of the thermal decomposition.

2. Experimental

2.1 Materials

Copper formate tetrahydrate (Kanto Chemical) as a copper source was dried at 80 ˚C for 6 h to obtain anhydrated copper formate (Cuf). Various amines with low boiling points were used as complexing agents: butylamine (b.p. 78 ˚C), pentylamine (b.p. 104 ˚C), and hexylamine (b.p. 132 ˚C). Octylamine (b.p. 176 ˚C) was used for comparison. These amines were purchased from TCI. All chemicals were used as received without further purification. Cuf was mixed with an amine by vigorous kneading with a spatula to obtain Cuf-amine complex ink. The molar ratio of amine to Cuf was 1.7 to 3.0.

Thermogravimetric (TG) analysis of the Cuf-amine complex inks was performed with various heating patterns under nitrogen gas using a TG–DTA 6300 (Seiko Instruments, Inc.) to determine the calcination temperature.

2.2 Fabrication of copper films

Prepared Cuf-amine complex ink was coated onto a square zone (15 x 15 mm) formed using masking tape with a thickness of 0.1 mm on a cleaned glass substrate using a squeegee.

The coated ink was calcined on a hot plate at 100 to 120 ˚C for 30 min after reaching the holding temperature at a heating rate of 5 ˚C/min under nitrogen gas at 4 L/min. After calcination, the temperature was decreased at 5 ˚C/min under nitrogen gas.

2.3 Characterizations of copper films

The resistivity of fabricated copper films was measured using a 4-point probe method (MCP-T600, Loresta-GP, Mitsubishi Kagaku), and the volume resistivity of the films was calculated from the measured resistivity and the thickness of the film based on measurements of a cross-section of the film using an optical micrograph (VHX-100, Keyence).

The crystallite structures of the prepared copper films were identified via X-ray diffraction (XRD, RINT 2200 V, Rigaku) with Cu Kα radiation.

The morphologies of the surfaces and cross-sections of the copper films were observed using field-emission scanning electron microscopy (FE-SEM, JEOL JSM6340F) at an accelerated voltage of 20 kV.

Thermogravimetry-mass spectrometry (TG-MS) of TG (TG8120, Rigaku) coupled with mass spectroscopy (M-QA200TS, Anelva) was used to analyze the process of thermal decomposition to produce the Cuf-amine complex inks.

3. Results and discussion

3.1 Thermal properties of complex inks

TG curves of complex inks of Cuf and various amines are shown in Fig. 1. The molar ratio of amine to Cuf was 2.0. The mass of all types of Cuf-amine complex inks was gradually decreased until approximately 120˚C, and linearly decreased until 150 ˚C. The mass loss yielded stable residues between 15 and 25 wt.% above 150 ˚C, which is comparable to the expected mass change in the conversion of $Cu(HCOO)_2(amine)_2$ to Cu. The complete

decomposition temperature of 160 ˚C applies to all types of Cuf-amine complex inks, which is much lower than that from Cuf alone (~240˚C), and indicates that the amine complexing ligands effectively assisted in the reduction of copper (II) [23,30–33]. The temperature for the onset of decomposition was indicated as intersection point between TG curves and horizontal dotted-line, occurred at 100 ˚C for Cuf-butylamine (b.p. 78 ˚C) ink, at 106 ˚C for Cuf-pentylamine (b.p. 106 ˚C) and Cuf-hexylamine (b.p. 132 ˚C) inks, and at 113 ˚C for Cuf-octylamine (b.p. 176 ˚C) ink. The decomposition onset temperature is related to the boiling point of an amine ink complex. Amines with a lower boiling point experience the onset of lower temperature in decomposition onset. Thus, temperatures of 100 to 120 ˚C were selected as the calcination temperatures to fabricate copper films.

3.2 Synthesis of copper films and characterization

Ink complexes made up of Cuf and various amines were calcined at temperatures ranging from 100 to 120 ˚C to produce copper films. The volume resistivities of copper films fabricated under various conditions are shown in Fig. 2. The error bars in the figure represent the max and min values. Copper film from a complex of Cuf-pentylamine ink showed a lower volume resistivity of approximately 20 μΩ cm when calcined at 110 to 120˚C. However, the resistivity was increased at 105 ˚C (Fig. 2b). Film calcined at 100˚C showed no conductivity. The film calcined from Cuf-butylamine at 110˚C showed high values for resistivity, although it showed low value at 115 and 120 ˚C (Fig. 2a). This was caused by the low boiling point of butylamine (b.p. 78˚C), which was evaporated before the finish of thermal decomposition. The film calcined from Cuf-hexylamine at 105˚C showed high values for resistivity, although it showed low value at 110 to 120 ˚C (Fig. 2c). This was caused by the high boiling point of butylamine (b.p. 132˚C), which was remained in the film. The film synthesized from Cuf-octylamine showed conductivity at 110 to 120 ˚C, but none below 105 ˚C (Fig. 2d).

The surface morphologies of copper films formed from complex inks with various Cuf-amine compositions and calcined at 110 ˚C are shown in Fig. 3. The amine to Cuf molar ratio was 2.0. The film calcined from Cuf-butylamine complex ink consisted of large particles (1 to 3 μm) with unstructured plates of approximately 500 nm (Fig. 3a). The film calcined from Cuf-pentylamine, Cuf-hexylamine, and Cuf-octylamine complex inks consisted of spherical particles with various sizes (Fig. 3, b, c, and d). The particle size distribution of the films calcined from Cuf-pentylamine consisted mostly of small particles of 100 to 200 nm with some larger particles. By contrast, the films calcined from Cuf-hexylamine and Cuf-octylamine complex inks consisted mostly of large particles of 300 to 500 nm and some small particles. The low resistivity of the film calcined from Cuf-pentylamine was caused by the tightly packing due to small particles formed in the gaps between the large particles.

The volume resistivity of the film calcined from Cuf-pentylamine inks with various molar ratios of pentylamine to Cuf at 110˚C for 30 min is shown in Fig. 4. The volume resistivity of the film calcined from ink with a ratio of 1.7 was high, but the film calcined from inks with ratios of 2.0 to 3.0 indicated lower resistivity, and the film calcined from ink with a ratio of 2.4 showed a resistivity of 5.7 μΩ cm, which was the lowest value. The theoretical ratio of amine to Cuf needed to form a complex ink is 2.0, as shown in Eq. 1.

$$Cu(HCOO)_2 + 2\ \text{amine} \rightarrow Cu(HCOO)_2(\text{amine})_2 \qquad (1)$$

The high resistivity of the film calcined from ink with a molar ratio of 1.7 was caused by insufficient decomposition due to insufficient complexing. The crystal structures and morphologies of the films were investigated to confirm the cause of the lowest value that was cited in the film calcined from complex ink with a molar ratio of 2.4.

Fig. 5 shows the XRD patterns of thin films calcined from complex inks of Cuf and pentylamine with various molar ratios of pentylamine to Cuf that ranged from 2.0 to 2.7. Sharp peaks corresponding to Cu could be observed in all films, and, thus, it was confirmed

that all complex inks with molar ratios of 2.0 to 2.7 were thermally decomposed to copper. The full width at half maximum of each peak of all films were quite similar, and there were no differences in the crystallinity of the films. The peaks of Cu were observed at 2θ=43.2˚, 50.3˚, and 73.9˚, which correspond to miller indexes of (111), (200), and (220), respectively (JCPDS 01-070-3038).

The surface morphologies of the films calcined from Cuf-pentylamine complex inks with molar ratios of 2.4 and 2.7 at 110 ˚C for 30 min are shown in Fig. 6. Film calcined from ink with a molar ratio of 2.0 (Fig. 3b) contained larger particles of 400 to 500 nm in addition to many small particles, and the gaps between the particles of the films calcined from complex ink with a molar ratio of 2.4 were the smallest of the three types of films. Fig. 7 shows the distribution of the particle sizes of the films from Cuf-pentylamine complex inks with molar ratios ranging from 2.0 to 2.7 calcined at 110˚C for 30 min. The particle sizes of each film show a different distribution. The film calcined from complex ink with a molar ratio of 2.0 showed a broad distribution of 100 to 400 nm. The film calcined from complex ink with a molar ratio of 2.4 showed a wider distribution and three peaks of 50-100, 300, and 500 nm. Some of the large particles (300-500 nm) were covered with small particles (50-100 nm). The particle size distribution of the film from complex ink with a molar ratio of 2.7 showed peaks of 50-250 and 400 nm, and the large particles were covered with small particles similar to the film from complex ink with a molar ratio of 2.4. As a result, the volume resistivity of the film calcined from complex ink with a molar ratio of 2.4 was the lowest, as shown in Fig. 4, since small particles were formed in the gaps between the large particles in the film.

3.3 Process for the formation of film from complex inks

The film synthesized from Cuf-amine complex ink consisted of spherical copper particles with various sizes (Fig. 7), which resulted in a lower volume resistivity of the film. The

process during the formation of copper particles in each film was analyzed via TG-MS. The decomposition process for Cuf-amine complexes has been reported by Farraj et al. who found that the thermal decomposition of Cuf proceeds in two stages, as illustrated by the following reactions and analyzed by the release of CO_2 or H_2 [35].

$$Cu(HCOO)_2 \rightarrow Cu(HCOO) + CO_2 + 1/2\ H_2 \quad (2)$$

$$Cu(HCOO) \rightarrow Cu + CO_2 + 1/2\ H_2 \quad (3)$$

Figs. 8 shows the CO_2 release by TG-MS analysis during the thermal decomposition of complex ink with various molar ratios of pentylamine to Cuf at 110 ˚C after a heating rate of 5˚C/min under nitrogen, which corresponds to Fig. 7. The color of ink during calcination can be divided into three durations: (I) blue color before reaction, (II) a color change to sky blue, and (III) a brown part that occurs in the sky blue ink. No CO_2 release was detected in each of the inks in duration (I), which indicated no reaction. In duration (II), CO_2 release started at 100 ˚C before reaching a setting temperature of 110 ˚C. The amount of CO_2 release was largely increased and then decreased after indicating the maximum value. In the duration, a sharp peak was observed in the complex inks with ratios of 2.4 (Fig. 8b) and 2.7 (Fig. 8c), however, two peaks were recognized in the ink with a ratio of 2.0 (Fig. 8a). In duration (III), the amount of CO_2 released was almost constant, followed by a gradual decrease. The times for constant CO_2 release differed for each ink. Almost the same amounts of CO_2 were released in durations (II) and (III), which accounts for the color of ink in the durations. The reaction of Cu^{2+} to Cu^{1+} shown in Eq. 2 occurred in duration (II), and the change from Cu^{1+} to Cu^0 occurred in duration (III) [35]. The difference between inks was predominantly the time of thermal decomposition in the duration, and the time for the complex ink with a molar ratio of 2.4 was the longest. The nucleation and growth of copper particles from the complex ink in each duration had a large affect on improvement in the conductivity of the copper film.

The process for the formation of copper particles during the calcination of Cuf and pentylamine complex ink is shown in Fig. 9. In the first stage, copper nuclei formed in the ink solution, which then grew to larger particles. The theoretical ratio for the formation of an amine-to-Cuf complex ink is 2.0 (Eq. 1), which might be insufficient for complexing. In duration (II) (Fig. 8a), two peaks were recognized in the ink reaction. This showed that the Cuf-amine complex reacted until the first peak, and then the amine that was unbonded by the reaction was again complexed with the Cuf alone, which caused the second peak. As the ratio of pentylamine to Cuf was increased from 2.0 to 2.4, Cuf was fully complexing in the ink. Furthermore, excess pentylamine acted as a solvent and increased the ratio from 2.4 to 2.7. For the complex inks with a ratio of 2.0, the nucleation of copper was slow because of the insufficient complexing of Cuf with an amount of amine as a solvent that was small, which resulted in fewer large particles (Fig. 7a). On the other hand, for complex inks with a ratio of 2.7, the complexing of Cuf with amine as a solvent was sufficient, which generated much copper nucleation that limited the growth of copper particles, although some large particles were recognized (Fig. 7c). For the complex inks with a ratio of 2.4, the nucleation and growth of copper particles was balanced, resulting in a good distribution of small to large particles (Fig. 7b). The decreased release of CO_2 in duration (III) might have generated smaller particles for each complex ink. Thus, a lower temperature fabrication at 110 ˚C was achieved via the selection of pentylamine and the selection of an amine to Cuf ratio of 2.4. One of the objectives in the lower temperature fabrication of copper conductive research is to fabricate copper conductive film or line on flexible substrate such as PET film, which has low heat resistance. In order to apply the developed complex ink and calcination condition to the flexible substrate, the technology development of adhesion to substrate to flexible substrate is further needed, which might be pre-treatment of substrate, because addition of substance into

the developed ink would be brought about high resistance of fabricated copper conductive film or line.

Conclusions

Strategy of lower temperature synthesis of copper conductive film from copper formate-amine complex ink was devised. Calcination temperatures was focused the decomposition onset temperature of copper formate-amine complex inks, and amines for complex ink were selected the ones with a low boiling point to avoid residue impurities after calcination. Complex inks using various types of amines, which were butylamine (b.p. 78 ˚C), pentylamine (b.p. 104 ˚C), and hexylamine (b.p. 132 ˚C), were calcined at 100 to 120 ˚C for 30 min under a nitrogen atmosphere, resulting in that the copper film calcined from copper-pentylamine complex ink showed the lowest values for resistivity. By varying the molar ratio of pentylamine to copper formate, an optimal ratio of 2.4 was established, and resulted in volume resistivity of 5.7 μΩ cm under calcination at 110 ˚C, which was 3.4 times that of bulk copper (1.7 μΩ cm). The copper film consisted mostly of three sizes of nanoparticles generated via a two-step formation process: 50-100, 300, and 500 nm. The low resistance was caused by tightly packing of small and large particles.

Declaration of interest: None.

This research did not receive any specific grant from funding agencies in the public, commercial, or not-for-profit sectors.

References

[1] M. Xu, D. Obodo, V.K. Yadavalli, The design, fabrication, and applications of flexible biosensing devices, Biosens. Bioelectron. 124–125 (2019) 96–114.

https://doi.org/https://doi.org/10.1016/j.bios.2018.10.019.

[2] R. Alrammouz, J. Podlecki, P. Abboud, B. Sorli, R. Habchi, A review on flexible gas sensors: From materials to devices, Sensors Actuators A Phys. 284 (2018) 209–231. https://doi.org/https://doi.org/10.1016/j.sna.2018.10.036.

[3] Y. Luo, D. Wu, Y. Zhao, Q. Chen, Y. Xie, M. Wang, L. Lin, L. Wang, D. Sun, Direct write of a flexible high-sensitivity pressure sensor with fast response for electronic skins, Org. Electron. 67 (2019) 10–18. https://doi.org/https://doi.org/10.1016/j.orgel.2019.01.001.

[4] Y. Han, J. Dong, Fabrication of self-recoverable flexible and stretchable electronic devices, J. Manuf. Syst. 48 (2018) 24–29. https://doi.org/https://doi.org/10.1016/j.jmsy.2018.04.011.

[5] T.R. de Oliveira, W.T. Fonseca, G. de Oliveira Setti, R.C. Faria, Fast and flexible strategy to produce electrochemical paper-based analytical devices using a craft cutter printer to create wax barrier and screen-printed electrodes, Talanta. 195 (2019) 480–489. https://doi.org/https://doi.org/10.1016/j.talanta.2018.11.047.

[6] S. Emamian, B.B. Narakathu, A.A. Chlaihawi, B.J. Bazuin, M.Z. Atashbar, Screen printing of flexible piezoelectric based device on polyethylene terephthalate (PET) and paper for touch and force sensing applications, Sensors Actuators A Phys. 263 (2017) 639–647. https://doi.org/https://doi.org/10.1016/j.sna.2017.07.045.

[7] Y. Sekertekin, I. Bozyel, D. Gokcen, A Flexible and Low-Cost Tactile Sensor Produced by Screen Printing of Carbon Black/PVA Composite on Cellulose Paper, Sensors . 20 (2020). https://doi.org/10.3390/s20102908.

[8] E. Carlos, J. Leppäniemi, A. Sneck, A. Alastalo, J. Deuermeier, R. Branquinho, R. Martins, E. Fortunato, Printed, Highly Stable Metal Oxide Thin-Film Transistors with Ultra-Thin High-κ Oxide Dielectric, Adv. Electron. Mater. 6 (2020) 1901071.

https://doi.org/10.1002/aelm.201901071.

[9] S. Qu, Y. Chen, W. Shi, M. Wang, Q. Yao, L. Chen, Cotton-based wearable poly(3-hexylthiophene) electronic device for thermoelectric application with cross-plane temperature gradient, Thin Solid Films. 667 (2018) 59–63. https://doi.org/https://doi.org/10.1016/j.tsf.2018.09.046.

[10] H. Yuan, T. Lei, Y. Qin, R. Yang, Flexible electronic skins based on piezoelectric nanogenerators and piezotronics, Nano Energy. 59 (2019) 84–90. https://doi.org/https://doi.org/10.1016/j.nanoen.2019.01.072.

[11] Y. Hu, Z. Zheng, Progress in textile-based triboelectric nanogenerators for smart fabrics, Nano Energy. 56 (2019) 16–24. https://doi.org/https://doi.org/10.1016/j.nanoen.2018.11.025.

[12] S.-B. Jeon, S.-J. Park, W.-G. Kim, I.-W. Tcho, I.-K. Jin, J.-K. Han, D. Kim, Y.-K. Choi, Self-powered wearable keyboard with fabric based triboelectric nanogenerator, Nano Energy. 53 (2018) 596–603. https://doi.org/https://doi.org/10.1016/j.nanoen.2018.09.024.

[13] C. Wu, T.W. Kim, T. Guo, F. Li, Wearable ultra-lightweight solar textiles based on transparent electronic fabrics, Nano Energy. 32 (2017) 367–373. https://doi.org/https://doi.org/10.1016/j.nanoen.2016.12.040.

[14] J. Kim, S. Byun, S. Lee, J. Ryu, S. Cho, C. Oh, H. Kim, K. No, S. Ryu, Y.M. Lee, S. Hong, Cost-effective and strongly integrated fabric-based wearable piezoelectric energy harvester, Nano Energy. 75 (2020) 104992. https://doi.org/https://doi.org/10.1016/j.nanoen.2020.104992.

[15] X. Li, K.H. Koh, M. Farhan, K.W.C. Lai, An ultraflexible polyurethane yarn-based wearable strain sensor with a polydimethylsiloxane infiltrated multilayer sheath for smart textiles, Nanoscale. 12 (2020) 4110–4118.

https://doi.org/10.1039/C9NR09306K.

[16] X. Xuan, H.S. Yoon, J.Y. Park, A wearable electrochemical glucose sensor based on simple and low-cost fabrication supported micro-patterned reduced graphene oxide nanocomposite electrode on flexible substrate, Biosens. Bioelectron. 109 (2018) 75–82. https://doi.org/https://doi.org/10.1016/j.bios.2018.02.054.

[17] Y.H. Kwak, W. Kim, K.B. Park, K. Kim, S. Seo, Flexible heartbeat sensor for wearable device, Biosens. Bioelectron. 94 (2017) 250–255. https://doi.org/https://doi.org/10.1016/j.bios.2017.03.016.

[18] Y. Lu, M.C. Biswas, Z. Guo, J.-W. Jeon, E.K. Wujcik, Recent developments in bio-monitoring via advanced polymer nanocomposite-based wearable strain sensors, Biosens. Bioelectron. 123 (2019) 167–177. https://doi.org/https://doi.org/10.1016/j.bios.2018.08.037.

[19] F. Cai, C. Yi, S. Liu, Y. Wang, L. Liu, X. Liu, X. Xu, L. Wang, Ultrasensitive, passive and wearable sensors for monitoring human muscle motion and physiological signals, Biosens. Bioelectron. 77 (2016) 907–913. https://doi.org/https://doi.org/10.1016/j.bios.2015.10.062.

[20] Y. Pang, J. Jian, T. Tu, Z. Yang, J. Ling, Y. Li, X. Wang, Y. Qiao, H. Tian, Y. Yang, T.-L. Ren, Wearable humidity sensor based on porous graphene network for respiration monitoring, Biosens. Bioelectron. 116 (2018) 123–129. https://doi.org/https://doi.org/10.1016/j.bios.2018.05.038.

[21] M. Hashem, A.A. Al Kheraif, H. Fouad, Design and development of wireless wearable bio-tooth sensor for monitoring of tooth fracture and its bio metabolic components, Comput. Commun. 150 (2020) 278–285. https://doi.org/https://doi.org/10.1016/j.comcom.2019.11.004.

[22] J. Li, T. Shi, C. Feng, Q. Liang, X. Yu, J. Fan, S. Cheng, G. Liao, Z. Tang, The novel

Cu nanoaggregates formed by 5 nm Cu nanoparticles with high sintering performance at low temperature, Mater. Lett. 216 (2018) 20–23. https://doi.org/https://doi.org/10.1016/j.matlet.2017.12.094.

[23] A. Yabuki, N. Arriffin, Electrical conductivity of copper nanoparticle thin films annealed at low temperature, Thin Solid Films. 518 (2010) 7033–7037. https://doi.org/10.1016/j.tsf.2010.07.023.

[24] C.H. Lee, C.-Y. Hyun, J.-H. Lee, Deposition of pure Cu films on glass substrates by decomposition of Cu complex pastes at 250 °C and additional Cu plating, Appl. Surf. Sci. 473 (2019) 359–365. https://doi.org/https://doi.org/10.1016/j.apsusc.2018.12.141.

[25] B. Lee, Y. Kim, S. Yang, I. Jeong, J. Moon, A low-cure-temperature copper nano ink for highly conductive printed electrodes, Curr. Appl. Phys. 9 (2009) e157–e160.

[26] S. Suren, W. Limkitnuwat, P. Benjapongvimon, S. Kheawhom, Conductive film by spray pyrolysis of self-reducing copper–silver amine complex solution, Thin Solid Films. 607 (2016) 36–42. https://doi.org/https://doi.org/10.1016/j.tsf.2016.03.040.

[27] B. Zhang, C. Chen, W. Li, J. Yeom, K. Suganuma, Well-Controlled Decomposition of Copper Complex Inks Enabled by Metal Nanowire Networks for Highly Compact, Conductive, and Flexible Copper Films, Adv. Mater. Interfaces. 7 (2020) 1901550. https://doi.org/10.1002/admi.201901550.

[28] W. Xu, T. Wang, Synergetic Effect of Blended Alkylamines for Copper Complex Ink To Form Conductive Copper Films, Langmuir. 33 (2017) 82–90. https://doi.org/10.1021/acs.langmuir.6b03668.

[29] Y. Dong, Z. Lin, X. Li, Q. Zhu, J.-G. Li, X. Sun, A low temperature and air-sinterable copper–diamine complex-based metal organic decomposition ink for printed electronics, J. Mater. Chem. C. 6 (2018) 6406–6415. https://doi.org/10.1039/C8TC01849A.

[30] A. Yabuki, S. Tanaka, Electrically conductive copper film prepared at low temperature by thermal decomposition of copper amine complexes with various amines, Mater. Res. Bull. 47 (2012) 4107–4111. https://doi.org/10.1016/j.materresbull.2012.08.052.

[31] A. Yabuki, N. Arriffin, M. Yanase, Low-temperature synthesis of copper conductive film by thermal decomposition of copper–amine complexes, Thin Solid Films. 519 (2011) 6530–6533. https://doi.org/10.1016/j.tsf.2011.04.112.

[32] A. Yabuki, S. Tanaka, Oxidation behavior of copper nanoparticles at low temperature, Mater. Res. Bull. 46 (2011) 2323–2327. https://doi.org/10.1016/j.materresbull.2011.08.043.

[33] A. Yabuki, Y. Tachibana, I.W. Fathona, Synthesis of copper conductive film by low-temperature thermal decomposition of copper–aminediol complexes under an air atmosphere, Mater. Chem. Phys. 148 (2014) 299–304.

[34] C. Paquet, T. Lacelle, B. Deore, A.J. Kell, X. Liu, I. Korobkov, P.R.L. Malenfant, Pyridine–copper(ii) formates for the generation of high conductivity copper films at low temperatures, Chem. Commun. 52 (2016) 2605–2608. https://doi.org/10.1039/C5CC07737K.

[35] Y. Farraj, M. Grouchko, S. Magdassi, Self-reduction of a copper complex MOD ink for inkjet printing conductive patterns on plastics, Chem. Commun. 51 (2015) 1587–1590. https://doi.org/10.1039/C4CC08749F.

Figure Captions

Fig. 1. TG curves of complex inks of copper formate (Cuf) and (a) butylamine, (b) pentylamine, (c) hexylamine, and (d) octylamine calcined at 5 ˚C/min under nitrogen. The molar ratio of amine to Cuf is 2.0.

Fig. 2. Volume resistivity of films from complex inks of Cuf and (a) butylamine, (b) pentylamine, (c) hexylamine, and (d) octylamine calcined at various temperatures for 30 min. The molar ratio of amine to Cuf is 2.0.

Fig. 3. Surface morphology of films from complex inks of Cuf and (a) butylamine, (b) pentylamine, (c) hexylamine, and (d) octylamine calcined at 110 ˚C for 30 min. The molar ratio of amine to Cuf is 2.0.

Fig. 4. Volume resistivity of films from complex inks of Cuf and pentylamine with various molar ratios of pentylamine to Cuf calcined at 110 ˚C for 30 min.

Fig. 5. XRD patterns of films calcined from complex inks of Cuf and pentylamine with various molar ratios of pentylamine to Cuf; (a) 2.0, (b) 2.4 and (c) 2.7 at 110˚C for 30 min.

Fig. 6. Surface morphologies of films calcined from complex inks of Cuf and pentylamine with various molar ratios of pentylamine to Cuf; (a) 2.4 and (b) 2.7 at 110˚C for 30 min.

Fig. 7. The distribution of particle size for films calcined at 110 ˚C for 30 min from complex inks of Cuf and pentylamine with various molar ratios of pentylamine to Cuf: (a) 2.0, (b) 2.4 and (c) 2.7.

Fig. 8. CO_2 release by MS analysis during thermal decomposition of complex ink of Cuf and pentylamine with a heating rate 5 ˚C/min under a nitrogen atmosphere with various molar ratios of pentylamine to Cuf: (a) 2.0, (b) 2.4 and (c) 2.7 at 110˚C.

Fig. 9. Formation process of copper particles during calcination of complex ink of Cuf and pentylamine.

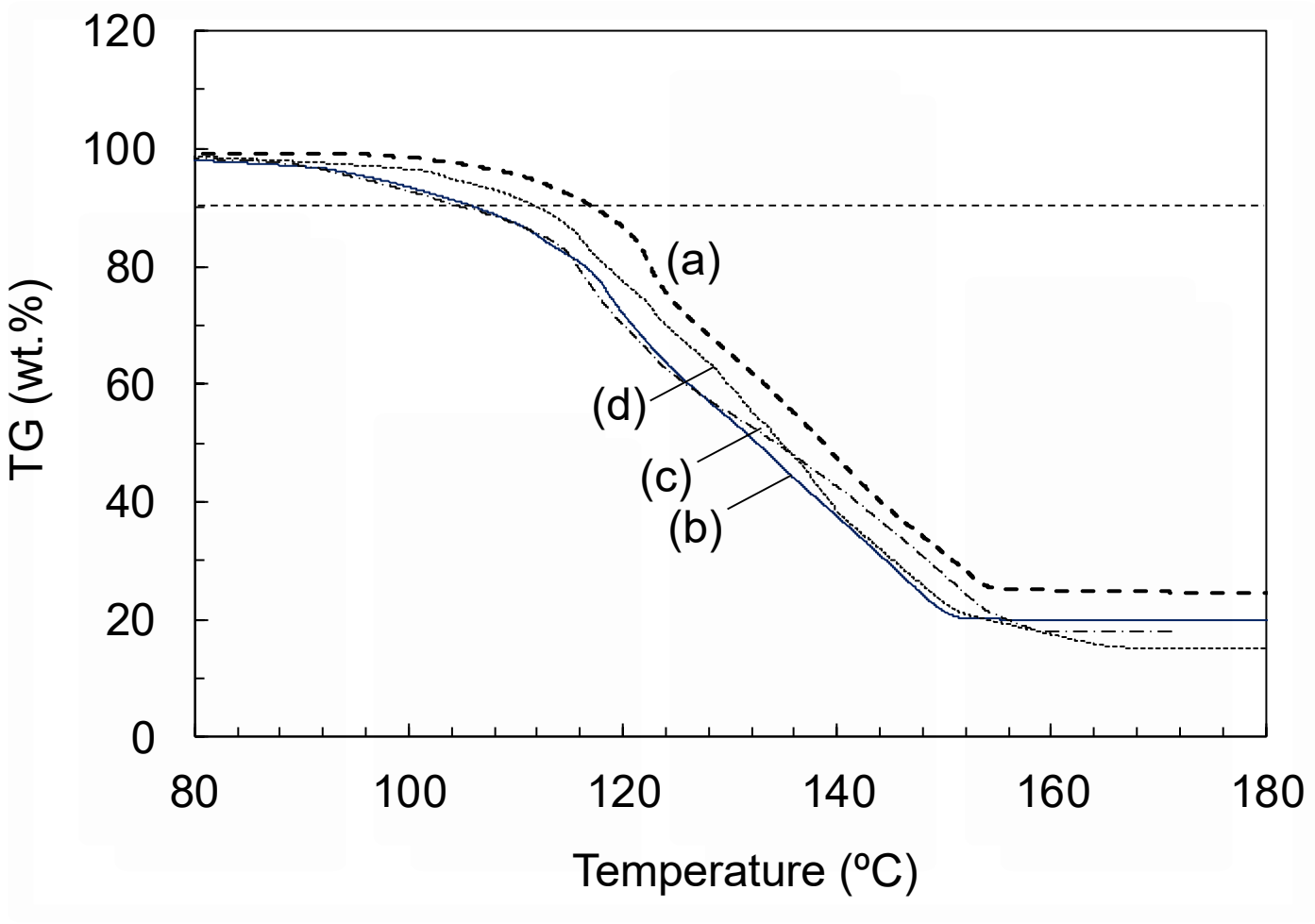

Fig. 1. Akihiro Yabuki et. al.

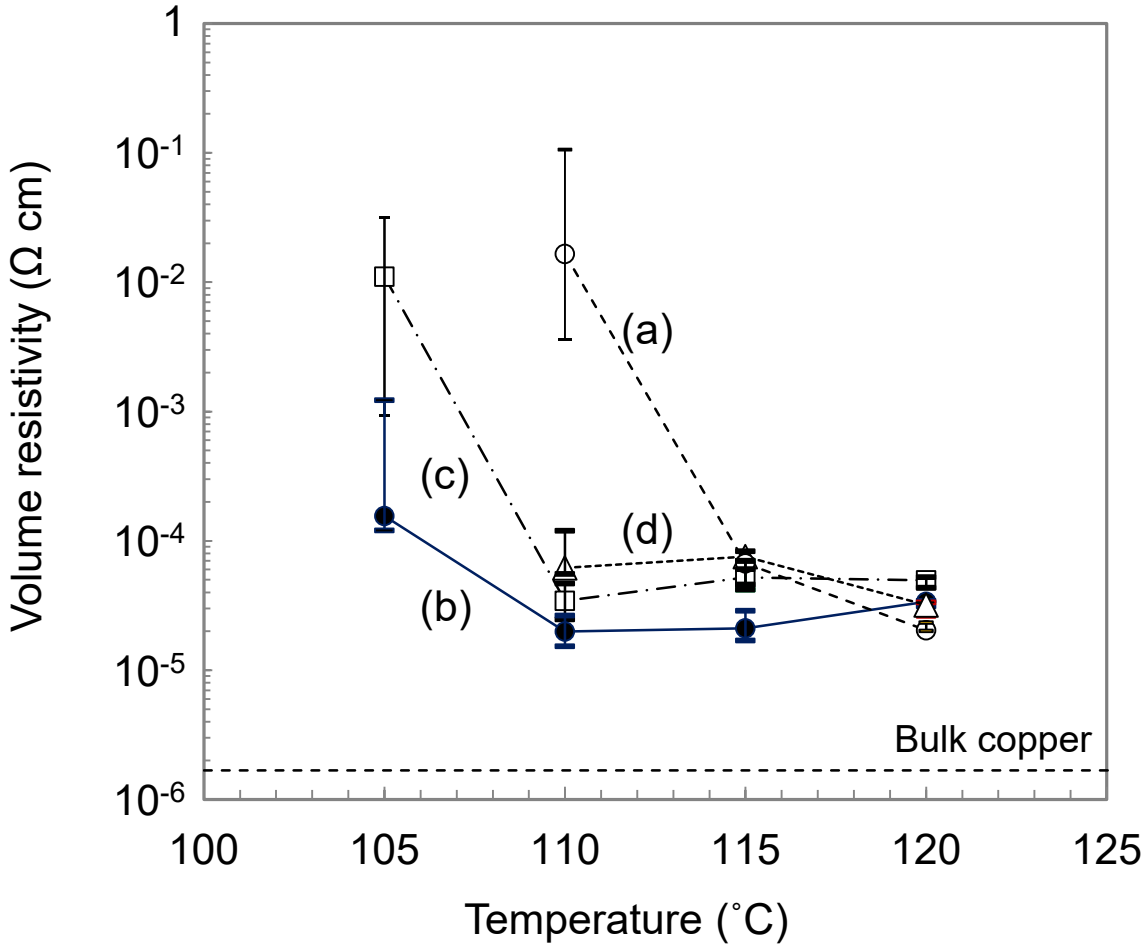

Fig. 2. Akihiro Yabuki et. al.

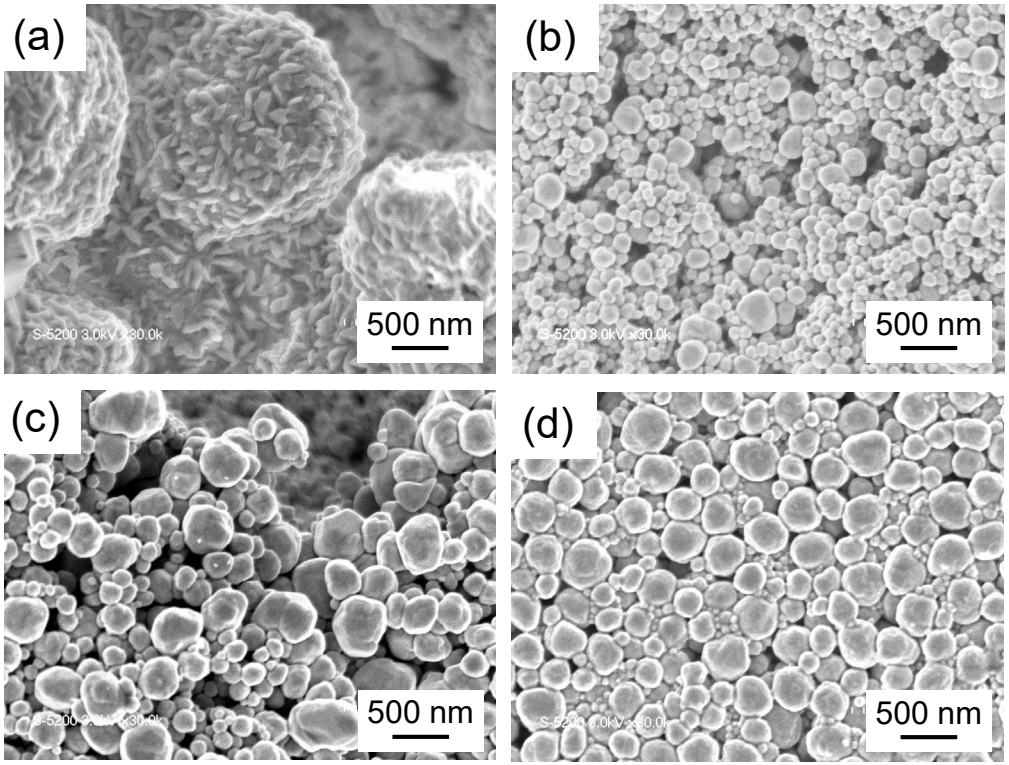

Fig. 3. Akihiro Yabuki et. al.

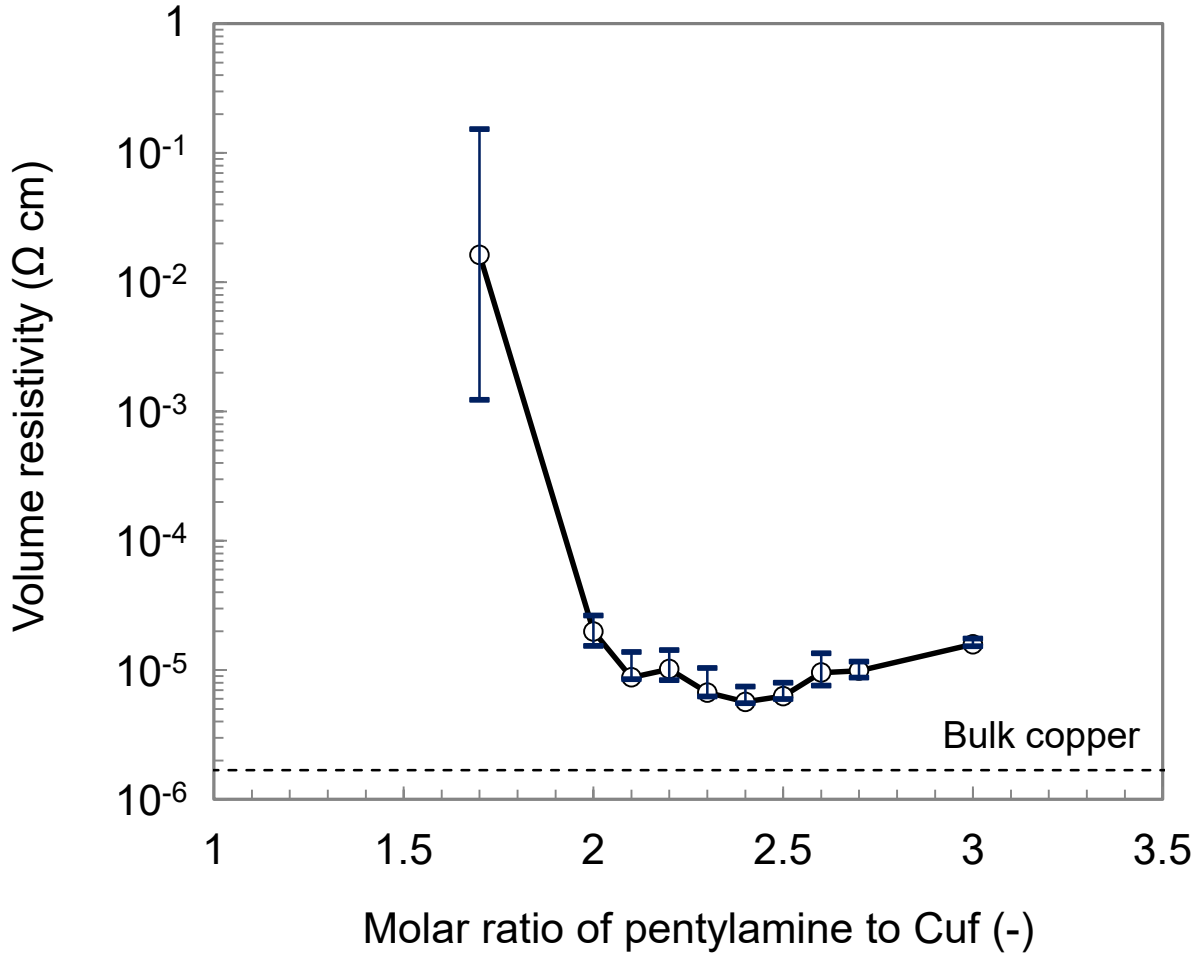

Fig. 4. Akihiro Yabuki et. al.

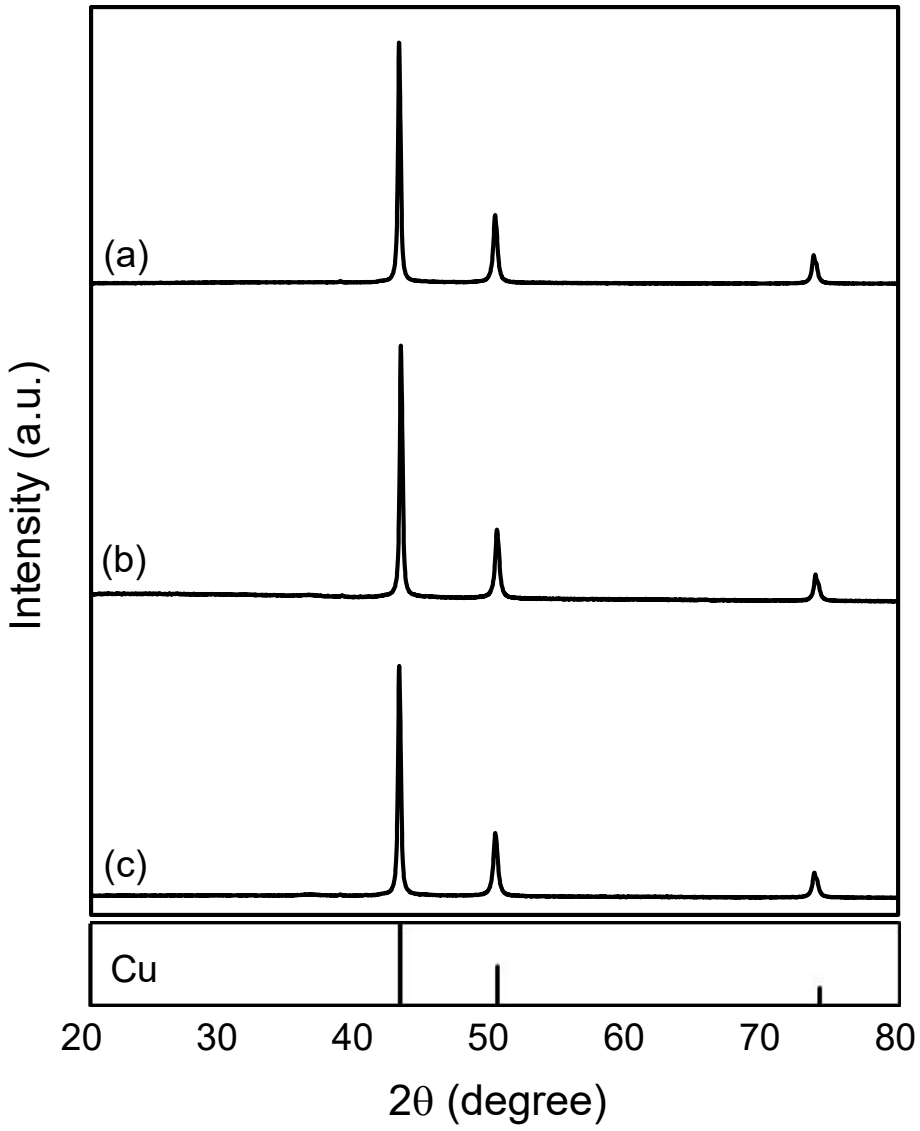

Fig. 5. Akihiro Yabuki et. al.

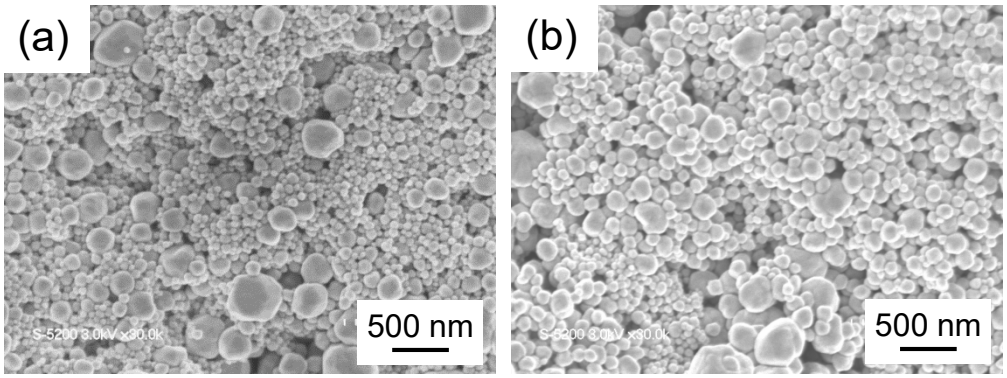

Fig. 6. Akihiro Yabuki et. al.

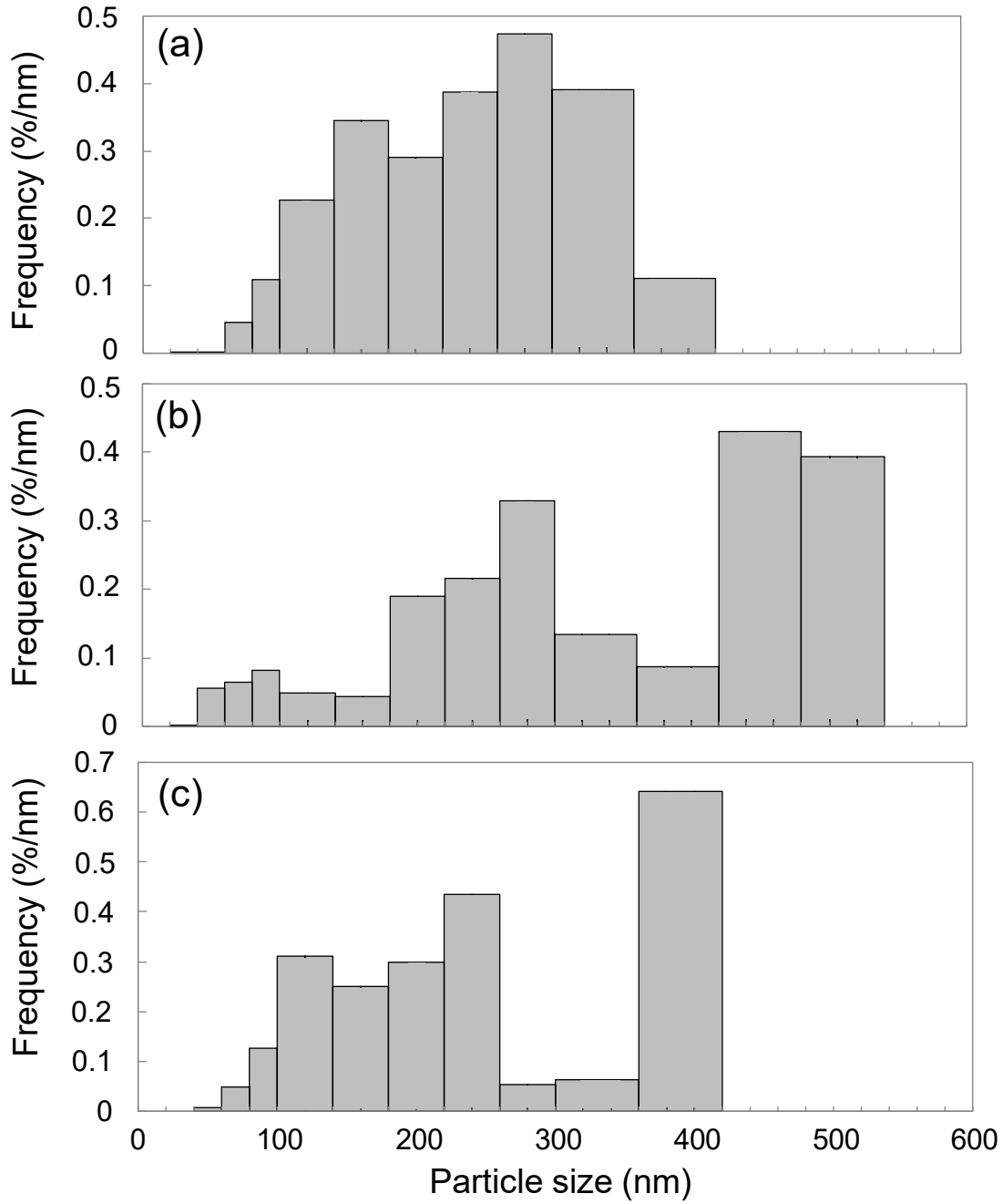

Fig. 7. Akihiro Yabuki et. al.

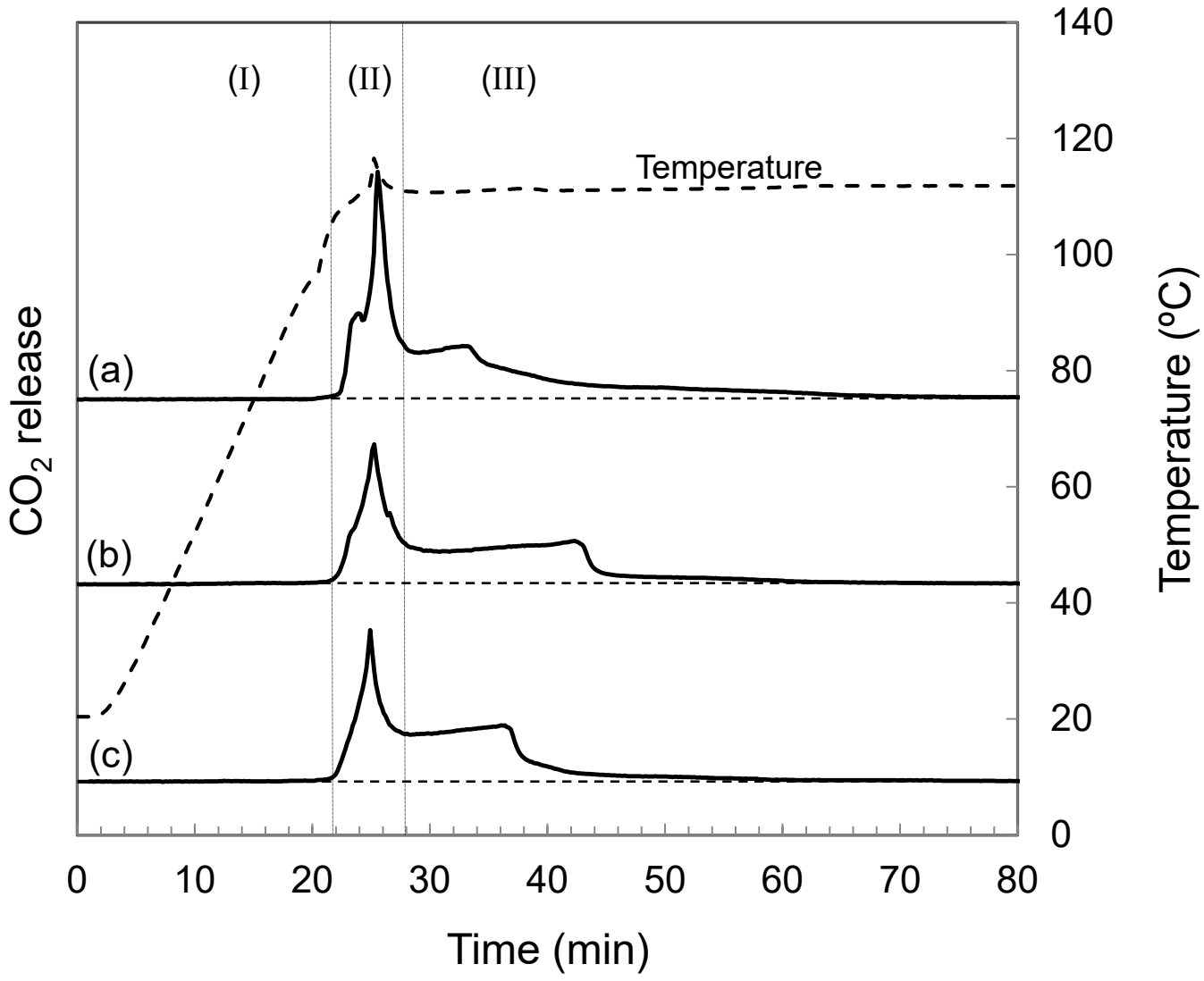

Fig. 8. Akihiro Yabuki et. al.

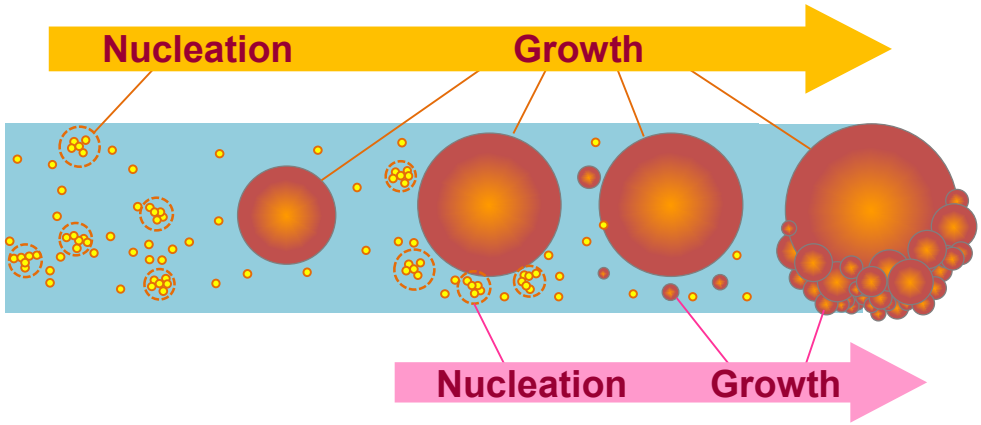

Fig. 9. Akihiro Yabuki et. al.